

Image-Based Material Decomposition with Energy-Selective Detectors in Multi-Energy CT: A Review

Marc Kachelrieß

German Cancer Research Center (DKFZ)

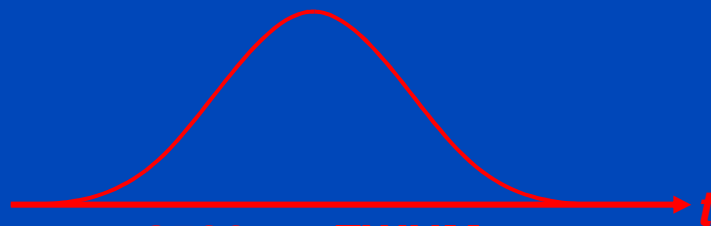
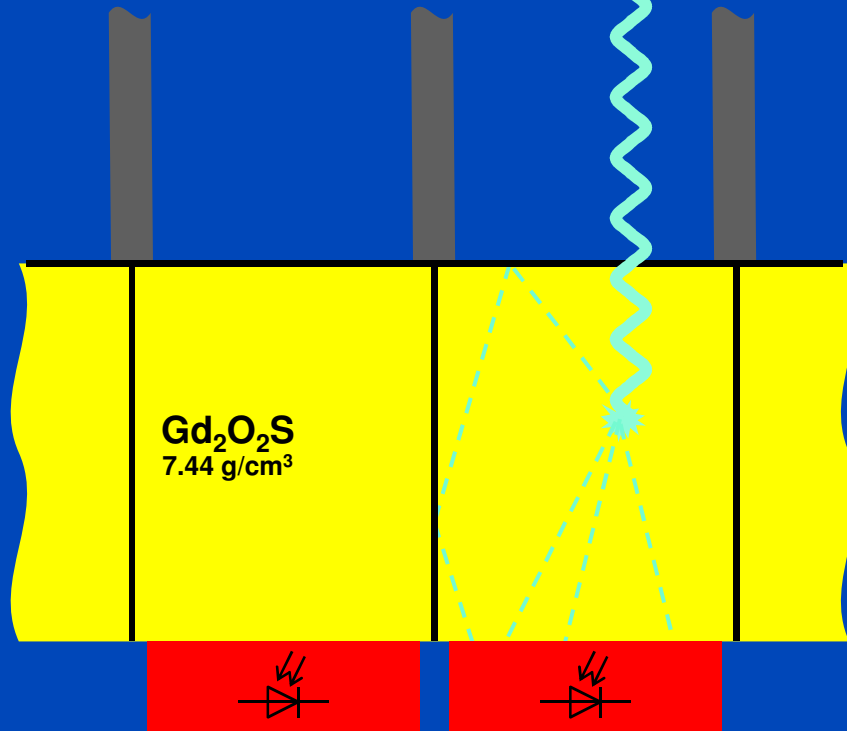
Heidelberg, Germany

www.dkfz.de/ct



DEUTSCHES
KREBSFORSCHUNGSZENTRUM
IN DER HELMHOLTZ-GEMEINSCHAFT

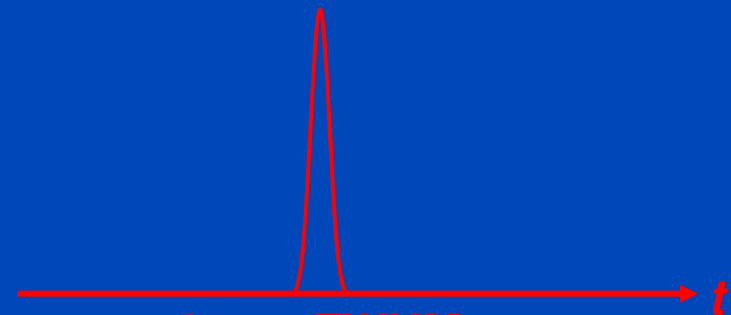
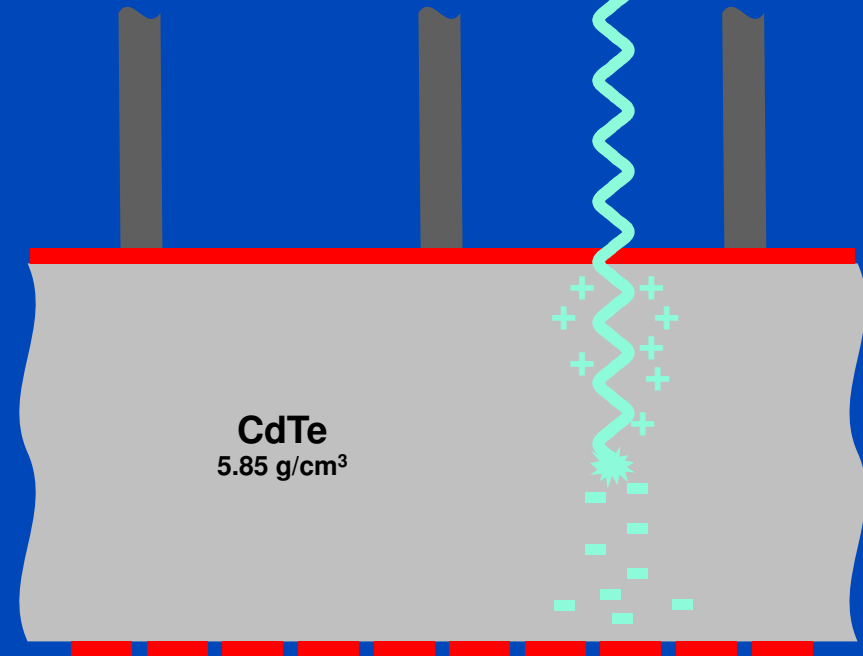
Indirect Conversion (Today)



2500 ns FWHM

i.e. max $\text{O}(40 \cdot 10^3)$ cps

Direct Conversion (Future)

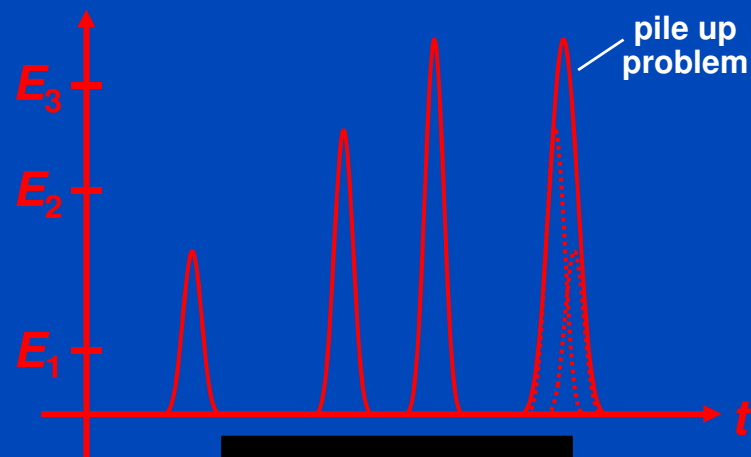
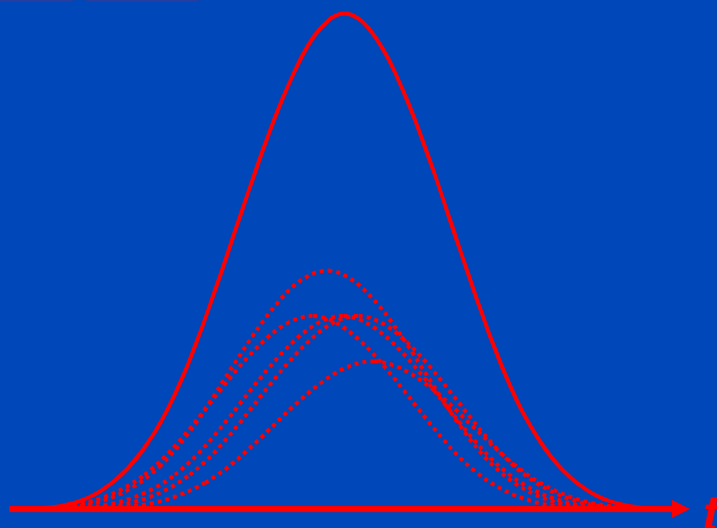
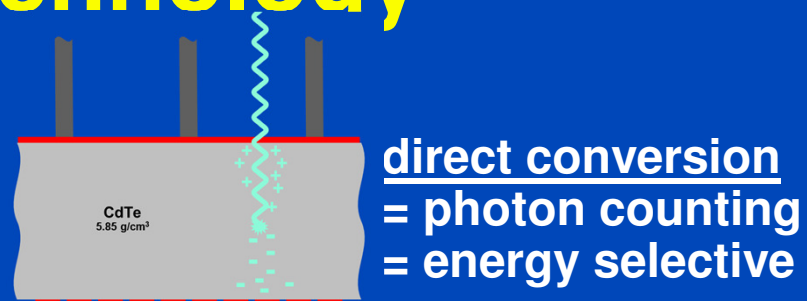
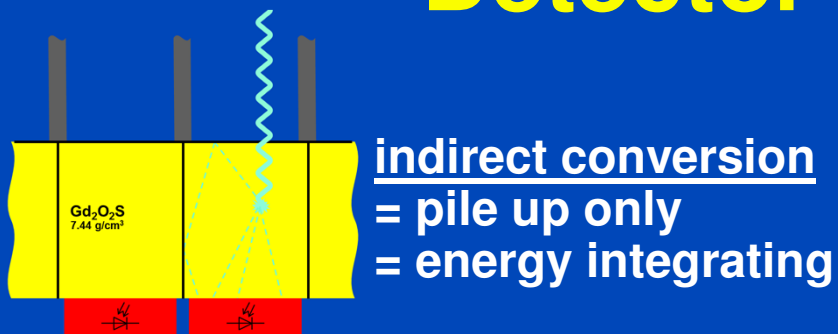


25 ns FWHM

i.e. max $\text{O}(40 \cdot 10^6)$ cps

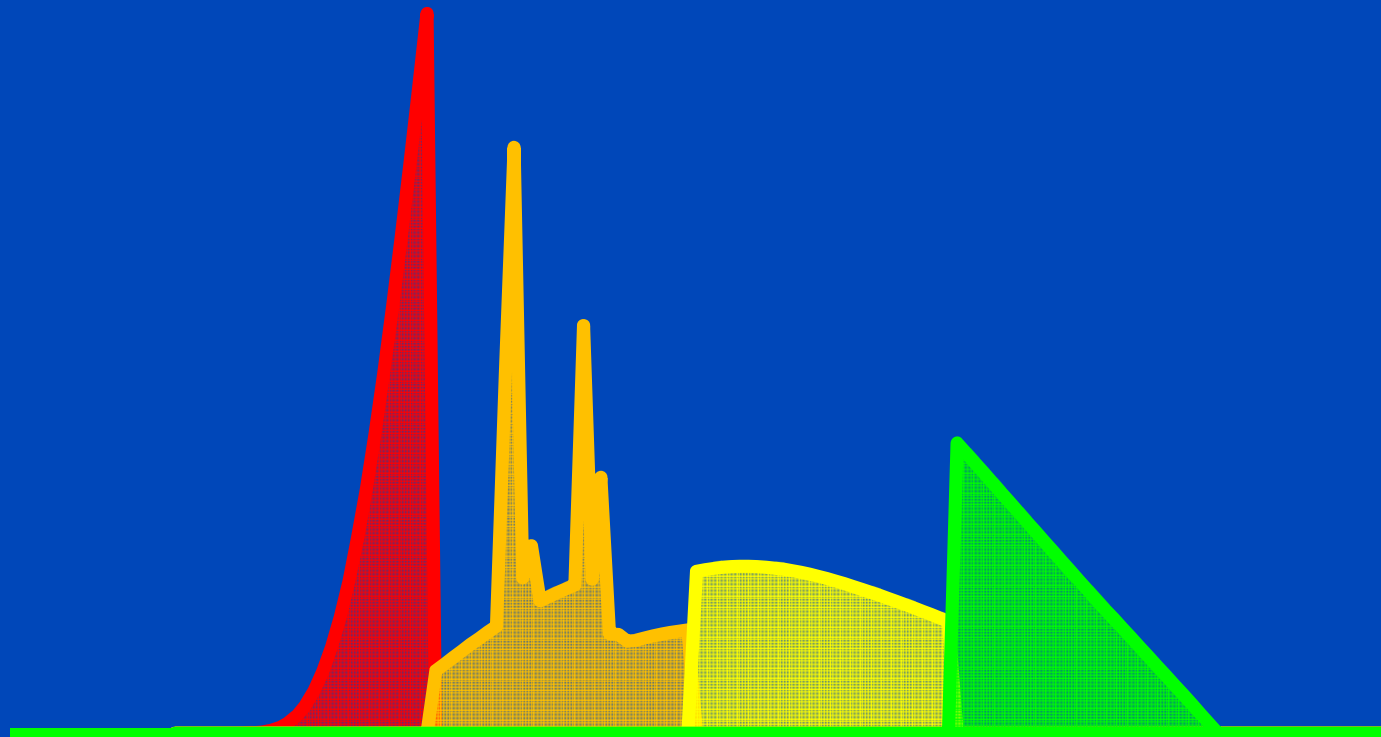
Requirements for CT: up to 10^9 x-ray photon counts per second per mm^2 .
Hence, photon counting only achievable for direct converters.

Integrating vs. Photon Counting Detector Technology



Energy Selective Detectors: Improved Spectroscopy, Reduced Dose?

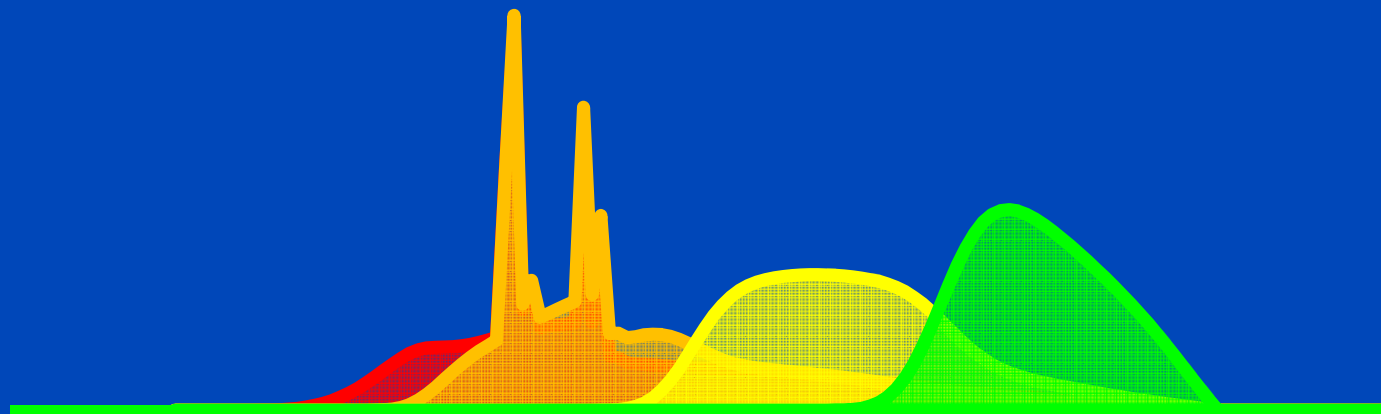
Ideally, bin spectra do not overlap, ...



Spectra as seen after having passed a 32 cm water layer.

Energy Selective Detectors: Improved Spectroscopy, Reduced Dose?

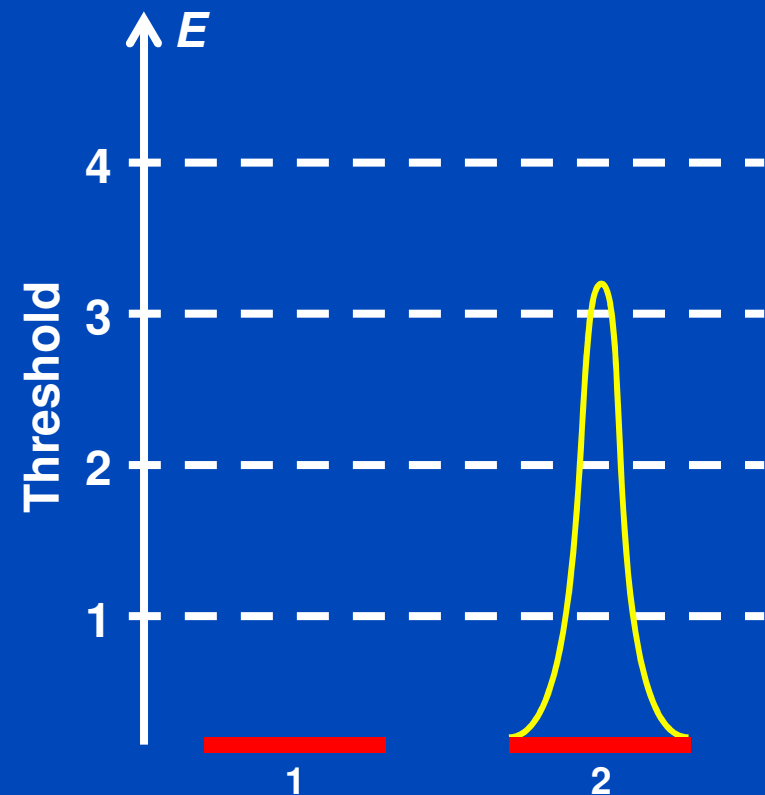
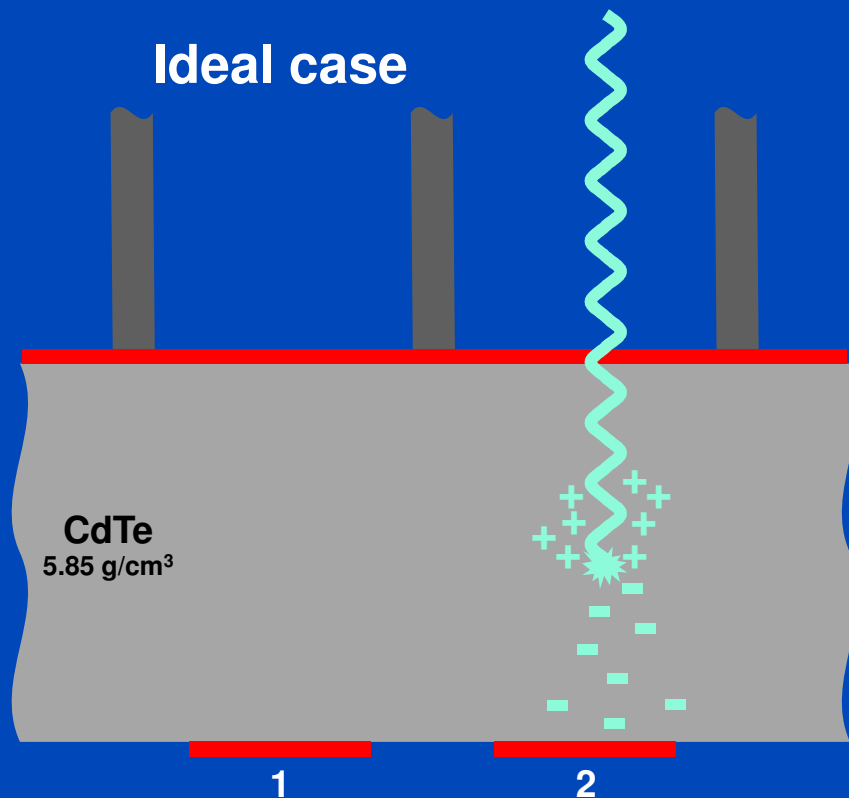
... realistically, however they do!



Spectra as seen after having passed a 32 cm water layer.

Photon Events

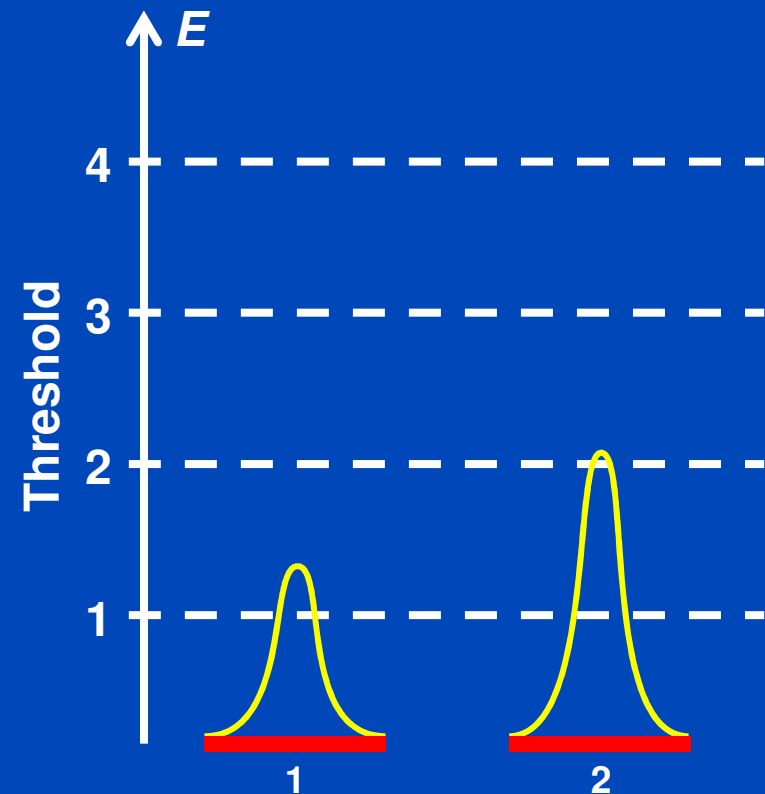
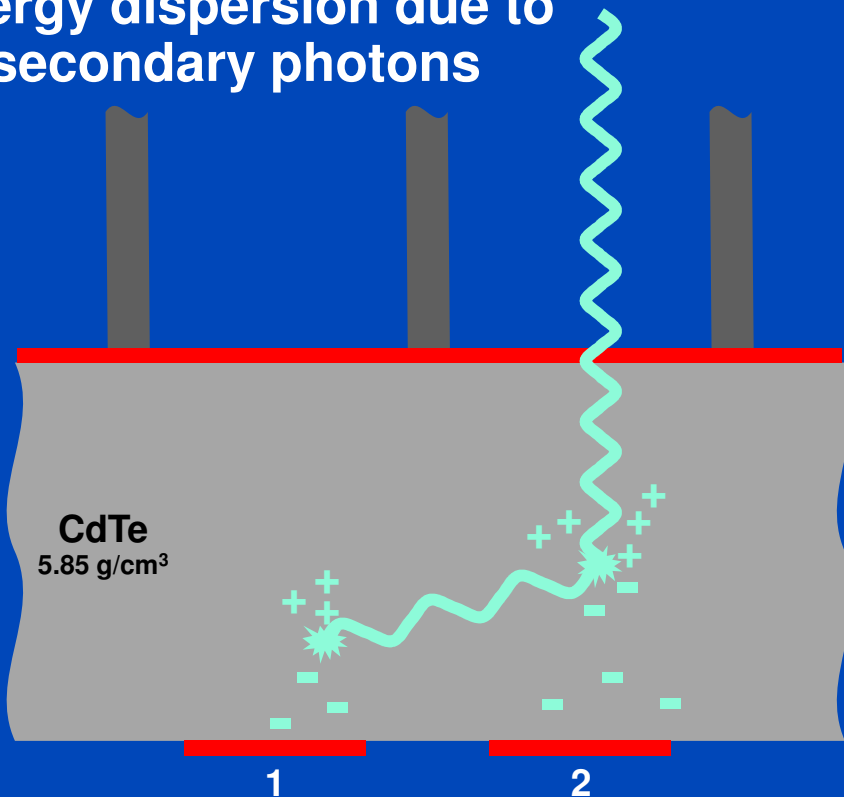
- Detection process in the sensor
- Photoelectric effect (e.g. 80 keV)



Photon Events

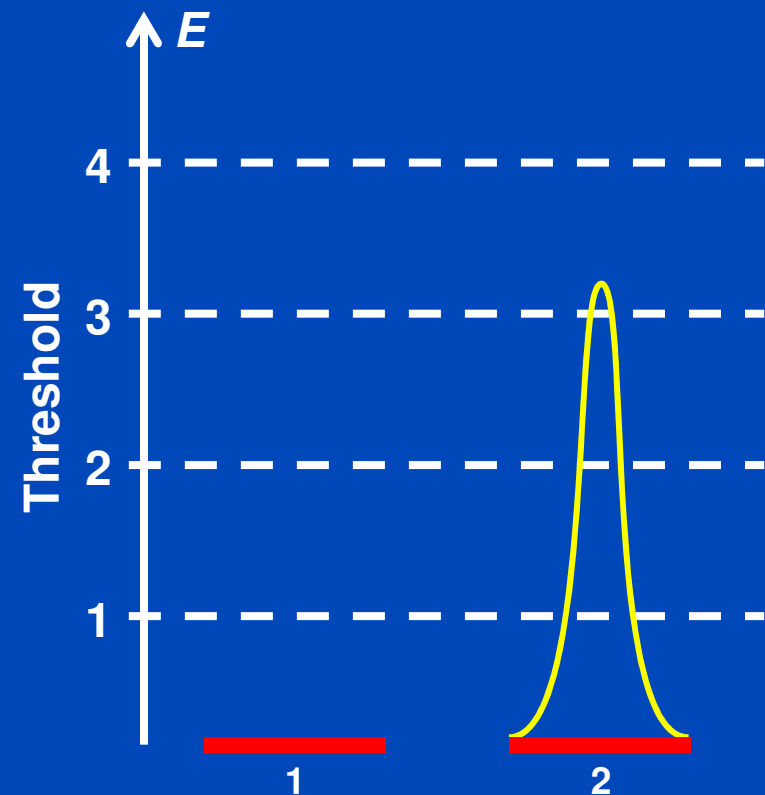
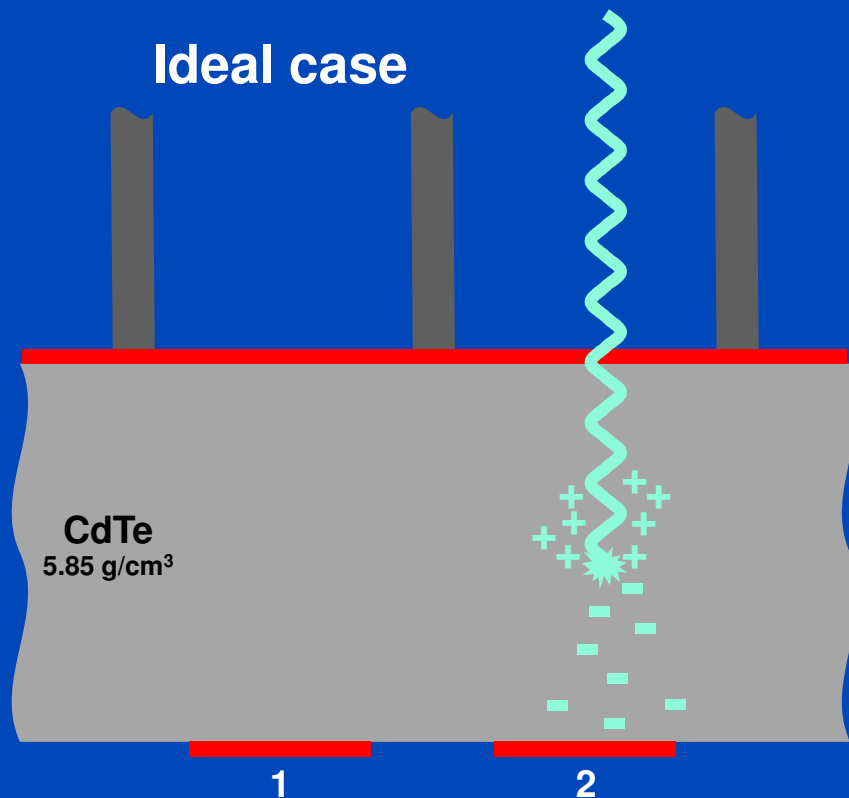
- Detection process in the sensor
- Compton scattering or K-fluorescence (e.g. 80 keV)

Energy dispersion due to secondary photons



Photon Events

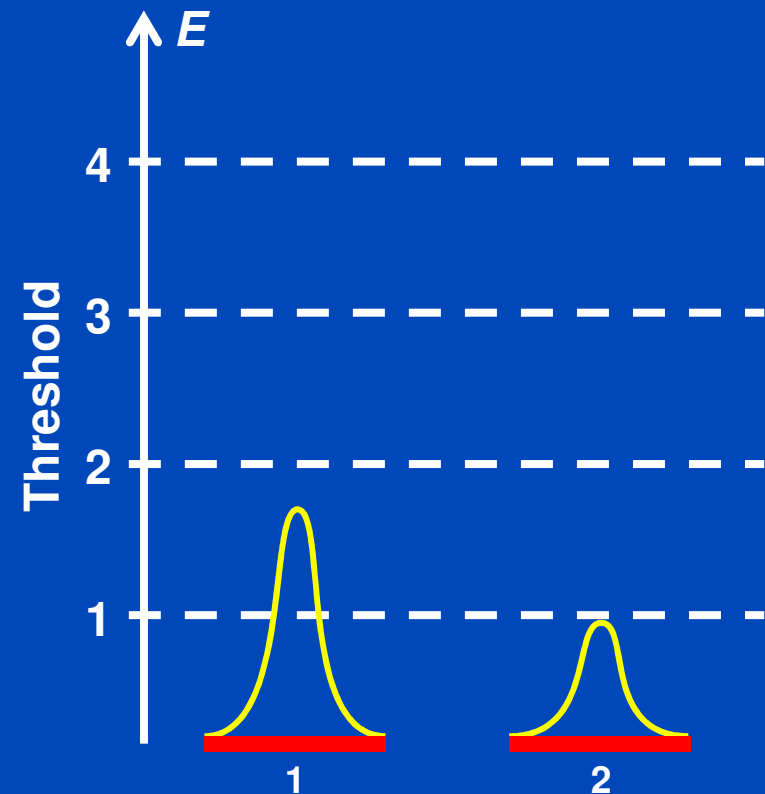
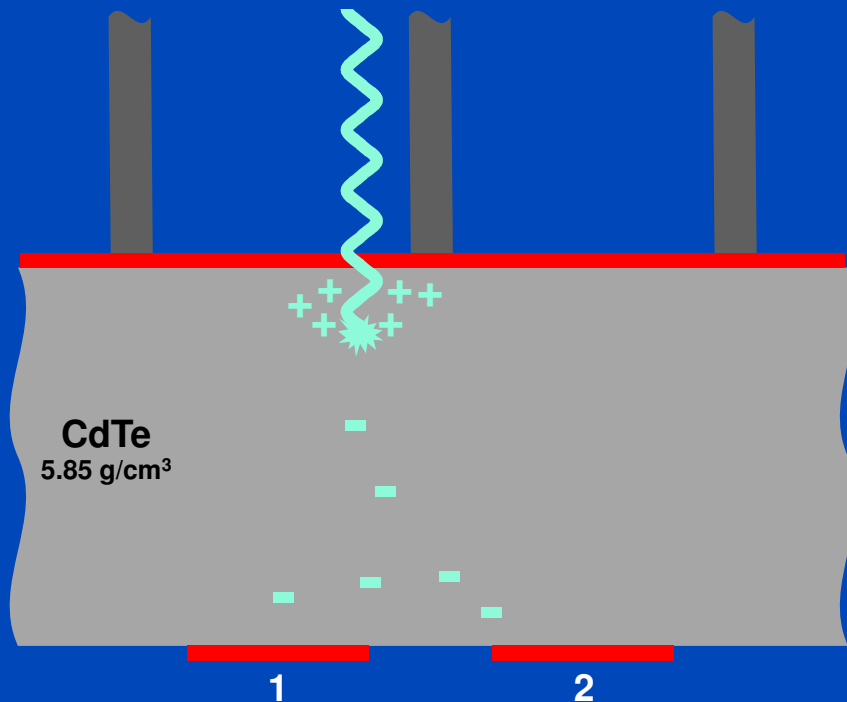
- Detection process in the sensor
- Photoelectric effect (e.g. 80 keV)



Photon Events

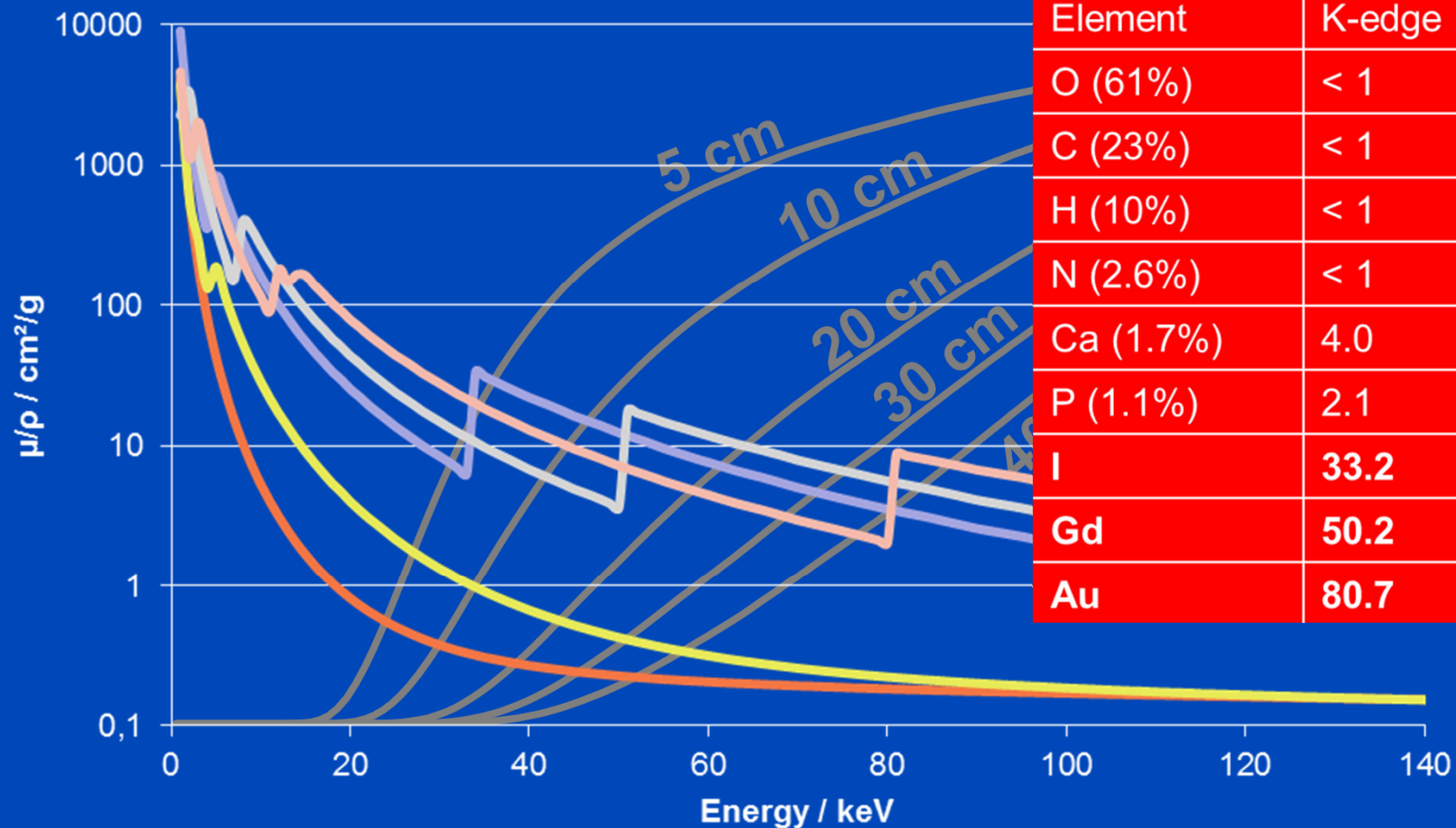
- Detection process in the sensor
- Photoelectric effect (e.g. 30 keV), charge sharing

Energy dispersion due to charge diffusion



K-Edges: More than Dual Energy CT?

$$\mu(\mathbf{r}, E) = f_1(\mathbf{r})\psi_1(E) + f_2(\mathbf{r})\psi_2(E) + f_3(\mathbf{r})\psi_3(E) + \dots$$



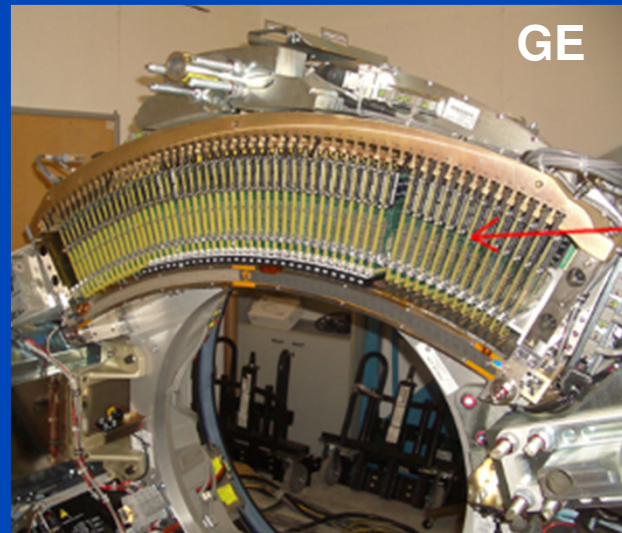
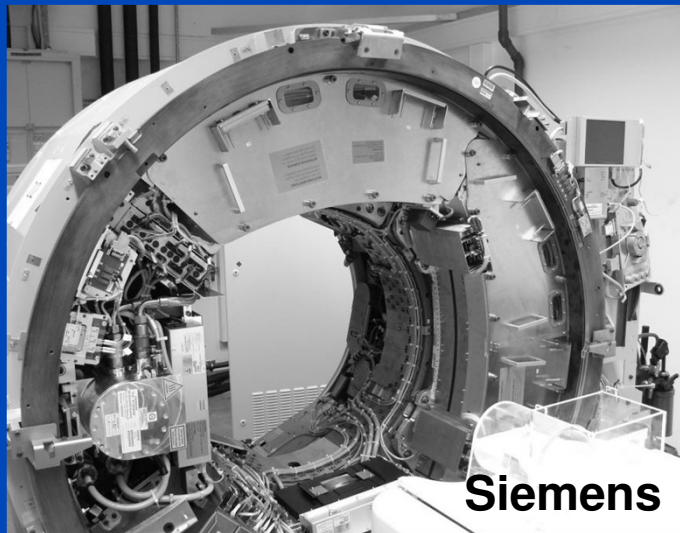
120 kV water transmission curves (gray) given in relative units on a non-logarithmic ordinate.

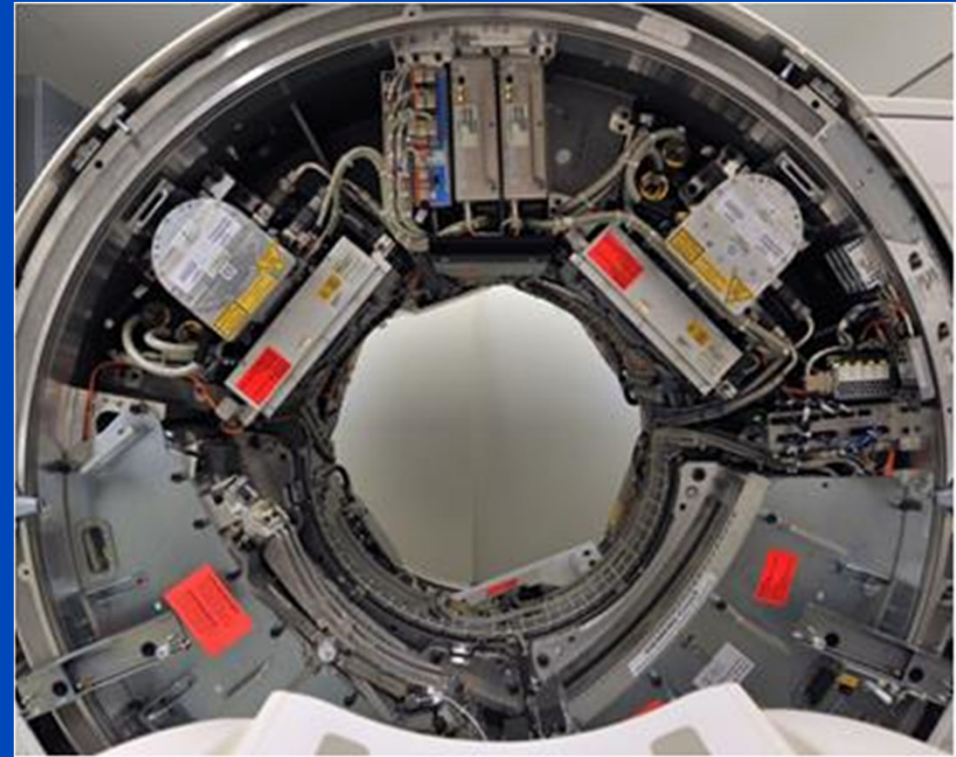
Remarks

- Photon counting is not necessarily energy-selective.
- Energy-selective CT
 - DECT
 - Photon-counting energy-selective detectors (i.e. at least two energy bins)
- DECT
 - DSCT
 - Fast TVS
 - Sandwich detector
 - Split filter
 - Two scans
- DECT or two bin photon-counting energy-selective CT can distinguish between more than two materials iff additional assumptions are made.

Aims

- Decompose MECT data in image domain
- Make use of energy data redundancies in multi energy CT
- Minimize noise in material images, i.e. reduce patient dose





This photon-counting whole-body CT prototype, installed at the Mayo Clinic, is a DSCT system. However, it is restricted to run in single source mode.

Motivation

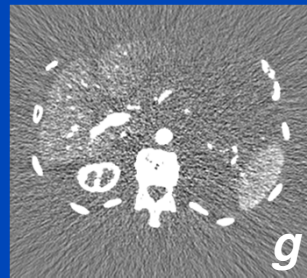
- **Without multiple high-Z contrast agents:**
- **Clinically interesting case only $M = 2$:**
 - Water/soft tissue and bone/iodine
 - Photoelectric effect and Compton scattering
- **Number energy bins $B >$ number basis materials M**
→ Gain in degrees of freedom, how to use it?
- **Image-based method for this task**
 - Narrow energy bins, images show only very little beam hardening
 - Linear image-based methods are fast.
- **Projection-based algorithms available**
 - Maximum likelihood approach (Roessl and Proksa, PMB 2007)
 - EMEC + Dose Min. (Maaß, Sawall, Knaup, and Kachelrieß, MIC 2011)

Algorithm Concept

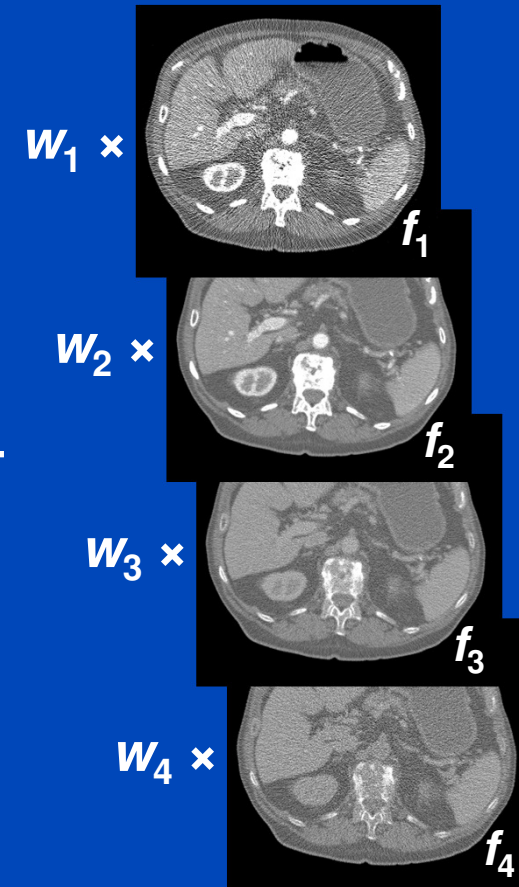
- Linear image weighting
 - Material image g
 - Weighting coefficients w
 - Energy bin images f

$$g = \begin{pmatrix} w_1 16.5 \\ +.81 8 \\ -.79 7 \\ w_B 4.9 \end{pmatrix} \begin{pmatrix} f_1 \\ f_2 \\ f_3 \\ f_4 \end{pmatrix}$$

Material image g



Bin images f



- Two subsequent steps:
 - Material decomposition calibration
 - Image noise minimization using the $K = B - M$ degrees of freedom

Material Decomposition Calibration

- Example for $M = 2$: water and iodine
- $N = 2$ calibration measurements using ROIs
- Determine weighting coefficients w
 - $M \times B$ coefficients, but $M \times N$ equations

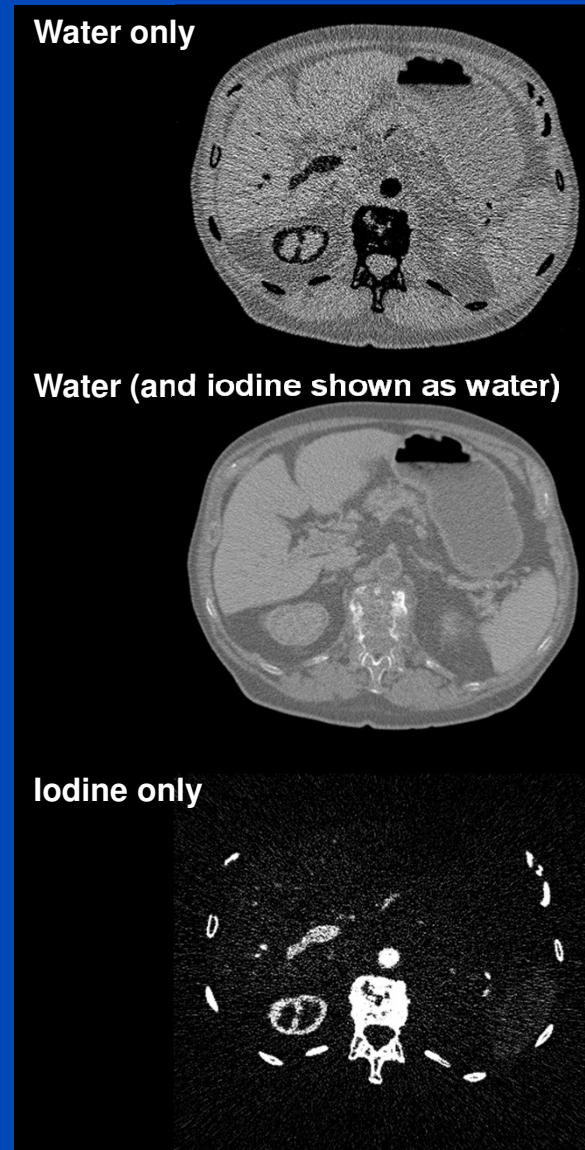
Water calibration
(maps water ROI values to target values):

$$\begin{pmatrix} \text{W-Image} \\ \text{I-Image} \end{pmatrix} = \begin{pmatrix} 1 \\ 0 \end{pmatrix} = \begin{pmatrix} w_{W,1} \dots w_{W,B} \\ w_{I,1} \dots w_{I,B} \end{pmatrix} \cdot \begin{pmatrix} f_{W,1} \\ \vdots \\ f_{W,B} \end{pmatrix}$$

Iodine calibration
(maps iodine ROI values to target values):

$$\begin{pmatrix} \text{W-Image} \\ \text{I-Image} \end{pmatrix} = \begin{pmatrix} 1 \\ 1 \end{pmatrix} = \begin{pmatrix} w_{W,1} \dots w_{W,B} \\ w_{I,1} \dots w_{I,B} \end{pmatrix} \cdot \begin{pmatrix} f_{I,1} \\ \vdots \\ f_{I,B} \end{pmatrix}$$

- This is the case studied in the following simulations



Material Decomposition Calibration

- Problem will now be treated separately for each of the the M basis materials, i.e. m is fixed
- $N \geq M$ calibration measurements to determine w :

$$g_n = \sum_b f_{nb} w_b \quad g = F \cdot w$$

- In general $N \neq B$, least squares approach:

$$w = \operatorname{argmin}_w (F \cdot w - g)^2$$

- Linear system for w :

$$\underbrace{F^T F}_{B \times B \text{ matrix, rank at most } M} \cdot w = \underbrace{F^T g}_{\text{Vector of dim. } B}$$

$B \times B$ matrix, rank at most M

Vector of dim. B

- Singular value decomposition:

$$w(\alpha_k) = w_0 + \sum_{k=1}^K \alpha_k w_k, \quad \forall \alpha_k \in \mathbb{R}$$

Rank M solution

Null space, dimension $K = B - M$

Image Noise Minimization

- Exploit free parameters α_k of the null space

$$w(\alpha_k) = w_0 + \sum_k \alpha_k w_k$$

- Noise minimization = maximizing CNR
- Covariance matrix C of all bin images:

$$C_{bb'} = \frac{1}{P-1} \sum_{p \in \text{ROI}} (f_b(p) - \bar{f}_b)(f_{b'}(p) - \bar{f}_{b'})$$

- Error propagation:

$$\text{Var } g = w^T(\alpha_k) \cdot C \cdot w(\alpha_k)$$

- Minimize variance: $\frac{\partial \text{Var } g}{\partial \alpha_j} = 0$

- Resulting linear system $A \cdot \alpha = b$ with:

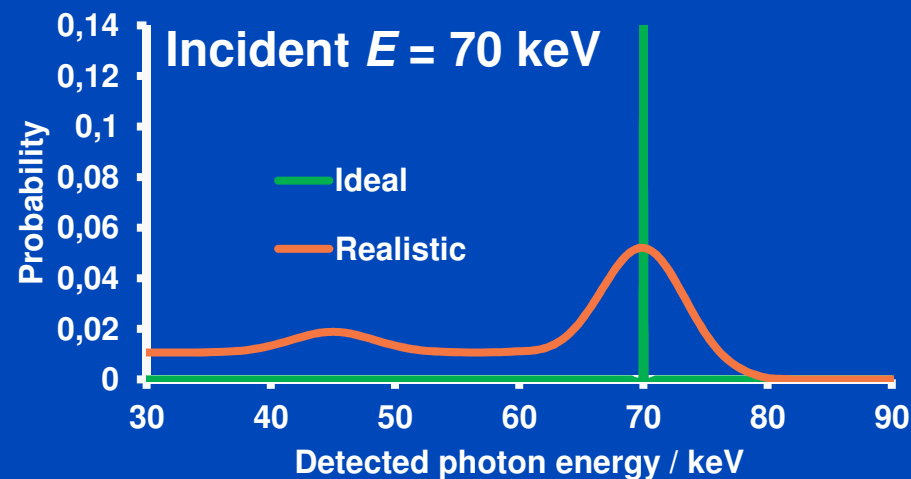
$$A_{jk} = \sum_b \sum_{b'} w_{jb} w_{kb'} C_{bb'} \text{ and } b_j = - \sum_b \sum_{b'} w_{jb} w_{0b'} C_{bb'}$$

Simulations

- **Assess the proposed algorithm**
- **Study a typical dual energy CT (DECT) application:**
 - Material decomposition into a water-equivalent virtual non-contrast (VNC) image and an iodine material image
- **Comparison of:**
 - Dual energy technique, energy integrating (EI) detectors
 - Energy-selective photon counting (PC) detectors
- **Based on patient data set with low noise**
 - Averaged over 8 thin slices
 - Separation into water and bone
 - Forward projection to obtain material-specific sinograms for polychromatic simulation

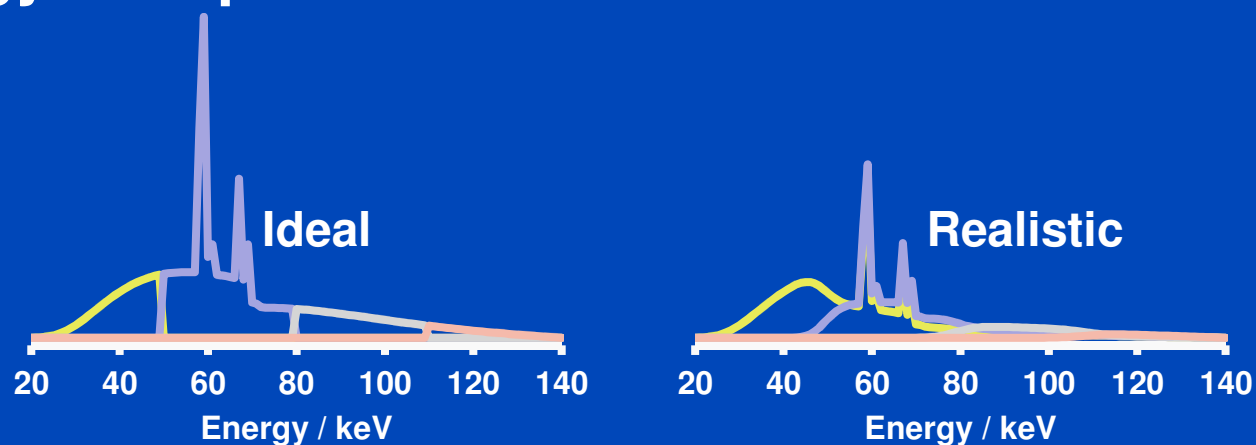
Simulations

- Spectral response:



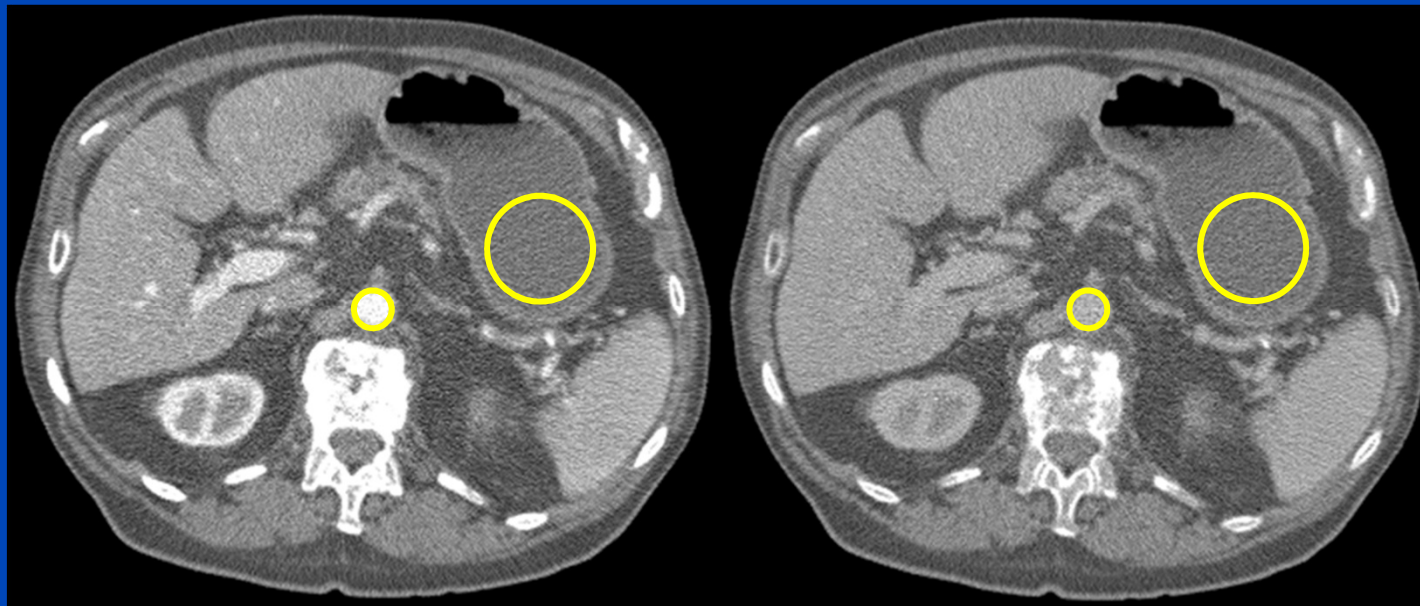
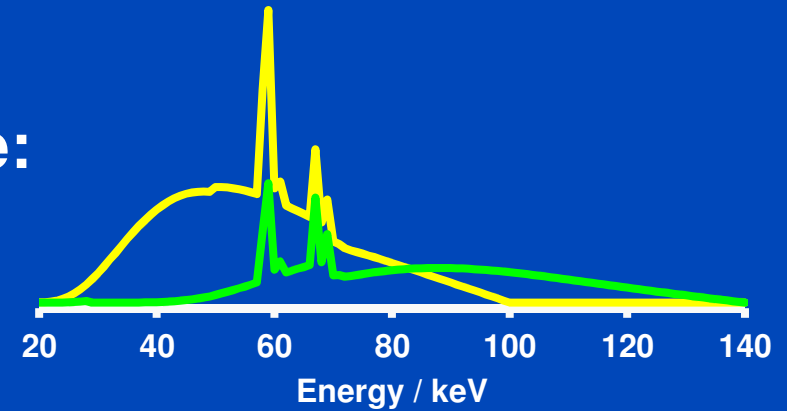
Energy bins placed equidistantly from 20 keV to 140 keV

- Energy bin spectra for $B = 4$:



Simulations

- Dual source DECT as reference:
 - 100 kV
 - 140 kV + 0.4 mm Sn



100 kV

140 kV Sn

$C = 0 \text{ HU} / W = 700 \text{ HU}$

Results – Ideal Model

DS 100 kV / Sn 140 kV

PC 2 bins

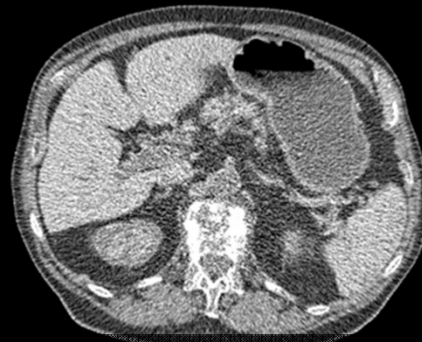
PC 4 bins

PC 8 bins

VNC



reference



-18% noise

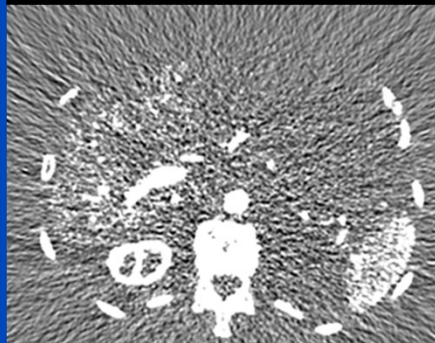


-24% noise

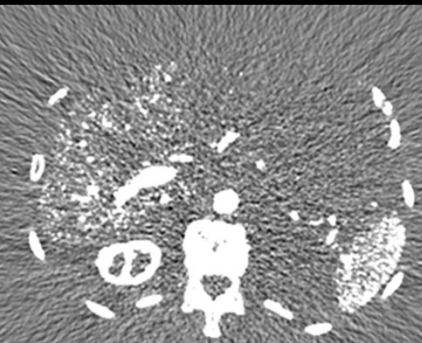


-29% noise

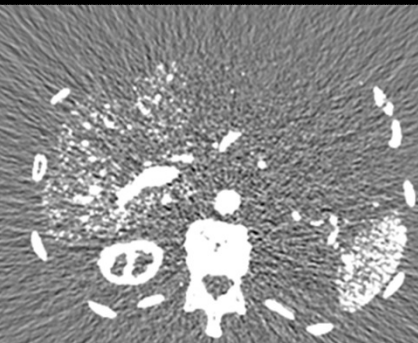
Iodine



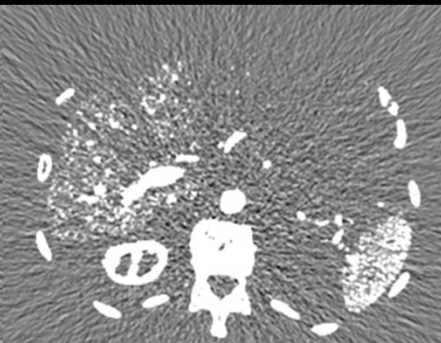
reference



-34% noise



-39% noise



-43% noise

$$\frac{\sigma_{PC}}{\sigma_{DECT}} = 1$$

For details regarding the material decomposition method see Faby *et al.*, SPIE 2014.

Water: $C = 0$ HU / $W = 400$ HU
Iodine: $C = 0$ mg/mL / $W = 6$ mg/mL

dkfz.

Results – PC (Realistic Model)

DS 100 kV / Sn 140 kV

PC 2 bins

PC 4 bins

PC 8 bins

VNC



reference



+21% noise

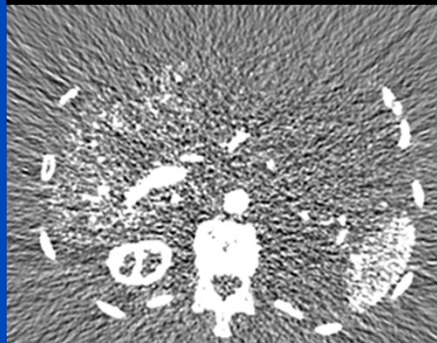


+15% noise

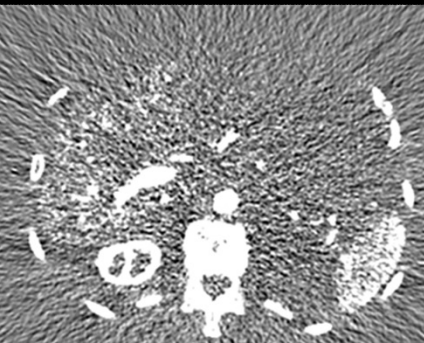


+9% noise

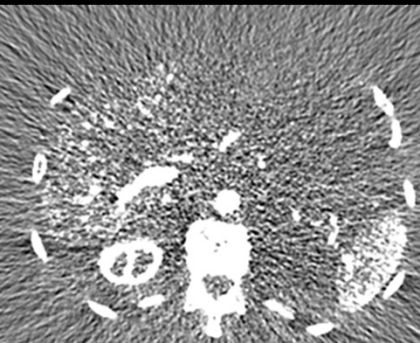
Iodine



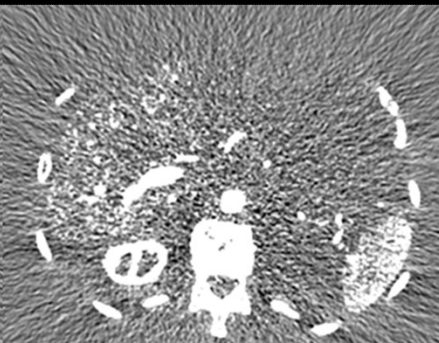
reference



+1% noise



-4% noise



-10% noise

$$\frac{\sigma_{PC}}{\sigma_{DECT}} = 1$$

For details regarding the material decomposition method see Faby *et al.*, SPIE 2014.

Water: $C = 0$ HU / $W = 400$ HU
 Iodine: $C = 0$ mg/mL / $W = 6$ mg/mL

dkfz.

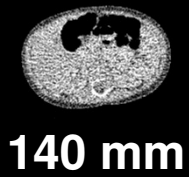
Patient-Specific Weighting

Small

Normal

Large

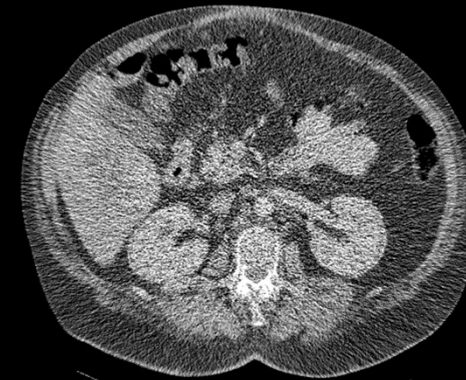
VNC



140 mm

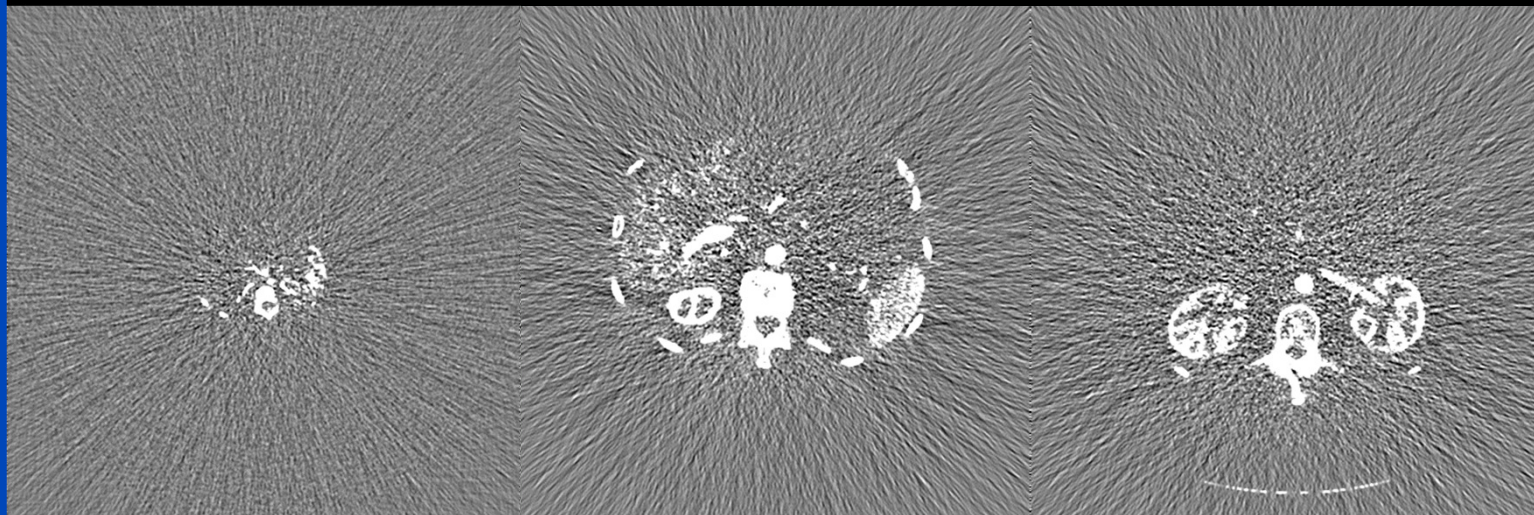


320 mm



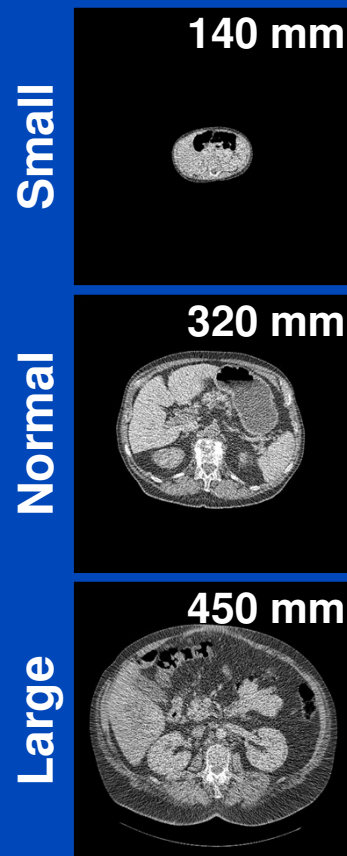
450 mm

Iodine



Patient-Specific Weighting

- Specifically optimized coefficients yield better results, especially for children.



Patient	Bins	VNC image noise		Iodine image noise	
		Std	Opt	Std	Opt
Small	2	0.0%	0.0%	0.0%	0.0%
	4	-5.3%	-9.5%	-6.5%	-11.5%
	8	-11.9%	-15.3%	-14.5%	-18.5%
Normal	2	0.0%	0.0%	0.0%	0.0%
	4	-4.7%	-4.7%	-5.1%	-5.1%
	8	-10.1%	-10.1%	-11.1%	-11.1%
Large	2	0.0%	0.0%	0.0%	0.0%
	4	-4.3%	-4.4%	-4.5%	-4.7%
	8	-9.3%	-9.5%	-9.9%	-10.1%

Simulation settings: 140 kV, realistic PC detector model

Selected Methods

**in chronological order and
in comparison to the initial method**

Optimal “image-based” weighting for energy-resolved CT

Taly Gilat Schmidt^{a)}

Department of Biomedical Engineering, Marquette University, Milwaukee, Wisconsin 53201

$$\text{CNR}_{\text{combined}} = \frac{\sum_{i=1}^M w_i \cdot C_i}{(\sum_{i=1}^M w_i^2 \cdot \sigma_i^2)^{1/2}}. \quad (6)$$

This paper considers how to combine the M energy-bin images in order to maximize the CNR of the final image. In the absence of noise, all of the weight would be given to the energy bin with the highest contrast (generally the low energy bin). In practice, the data from the lowest energy bin are generally noisiest because of the small number of detected photons.

The derivative of the CNR of the combined image with respect to the weight of the n th energy bin w_n is

$$\frac{\partial \text{CNR}_{\text{combined}}}{\partial w_n} = \frac{C_n \cdot \sum_{i=1}^M w_i^2 \sigma_i^2 - w_n \sigma_n^2 \cdot \sum_{i=1}^M w_i C_i}{(\sum_{i=1}^M w_i^2 \cdot \sigma_i^2)^{3/2}}. \quad (7)$$

A solution to this optimization problem is to weight each image proportionally to CNVR. For example, the weight of the n th energy-bin image is

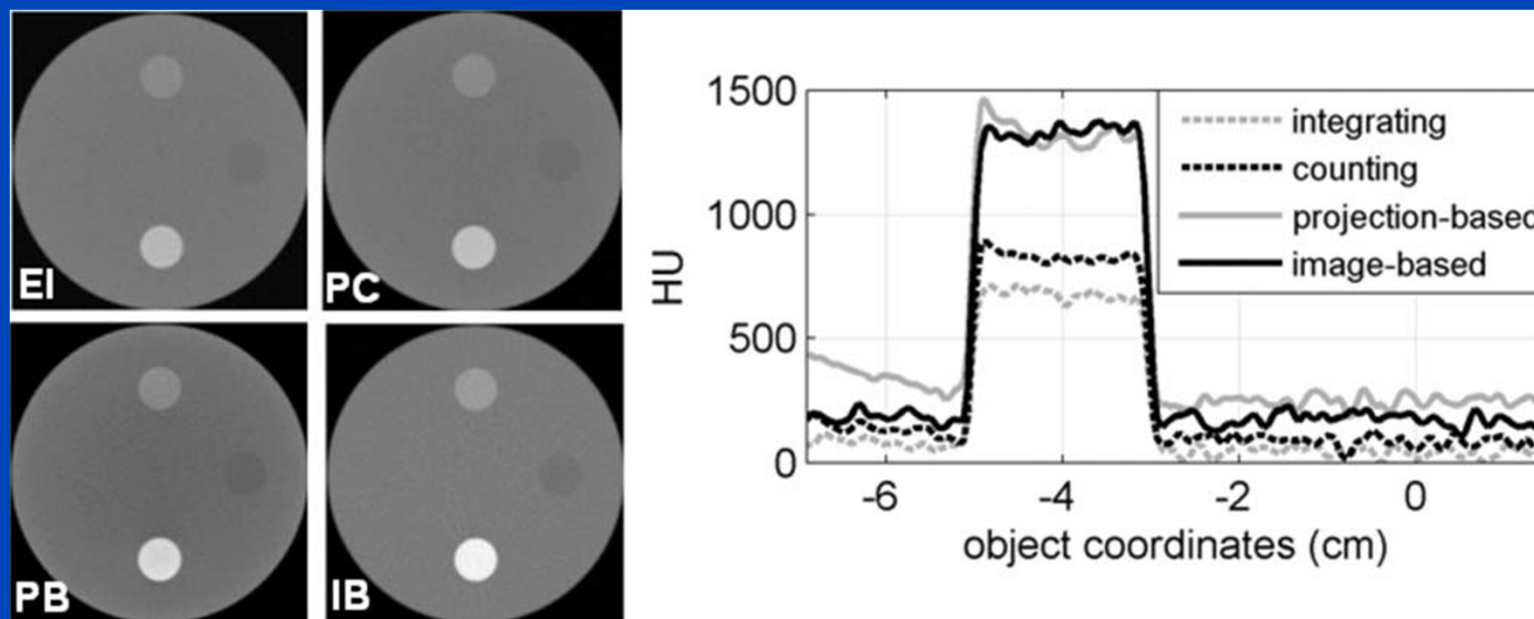
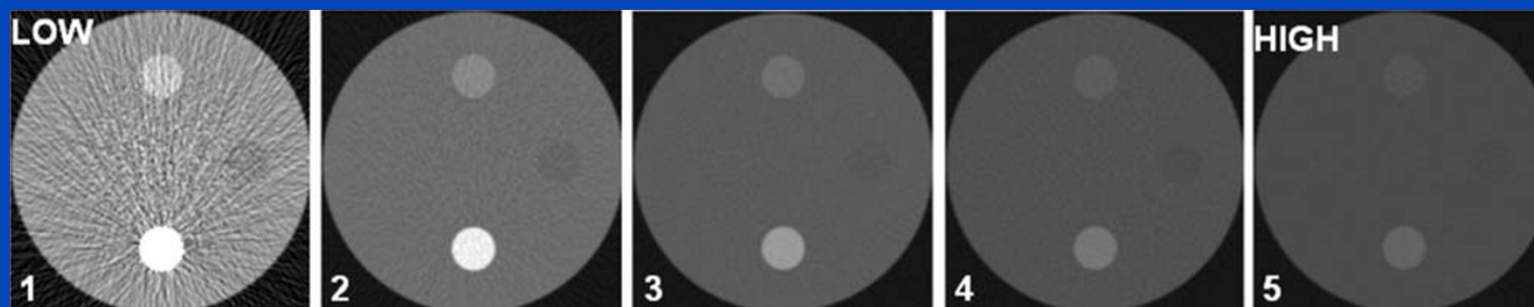
$$w_n \propto \frac{C_n}{\sigma_n^2}. \quad (8)$$

Optimal “image-based” weighting for energy-resolved CT

Taly Gilat Schmidt^{a)}

Department of Biomedical Engineering, Marquette University, Milwaukee, Wisconsin 53201

Results for $B = 5$



Comparison to Initial Method

- No material decomposition, only CNR optimization
- Comparable to the initial method's noise minimization step (without the calibration)
- Important difference to the initial method's noise minimization:
The weighting coefficients here do not take the covariance into account, but only the variance of the energy-resolved images. This might be sufficient for energy bin images, but surely not for threshold images.

Multi-energy performance of a research prototype CT scanner with small-pixel counting detector

S. Kappler^{a*}, A. Henning^a, B. Krauss^a, F. Schoeck^a,
K. Stierstorfer^a, T. Weidinger^a, and T. Flohr^a

^aSiemens Healthcare, Siemensstr. 1, 91301 Forchheim, Germany.

In our approach we request the following relation between the spectral images I_n and the material decomposed images J_m :

$$I_n = \sum_{m=1}^M \frac{c_{mn}}{c_{m0}} \cdot J_m \quad (1)$$

$$\vec{I} = U \cdot \vec{J} \quad (2)$$

In the case $M = N$, where U is a square matrix, the material images can be computed directly by inversion of the matrix U :

$$\vec{J} = U^{-1} \cdot \vec{I} \quad (3)$$

For $M < N$ the system of equations is over-determined. We chose the following approach to solve this problem. We choose M spectral images in all possible combinations out of the N recorded data sets.

This yields $K = \binom{N}{M}$ sets of images \vec{I}^k (with $k = 1 \dots K$) and decomposes the $M \times N$ matrix U into K square $M \times M$ matrices U^k . From each of these matrices the corresponding material images \vec{J}^k can be computed by matrix inversion:

$$\vec{J}^k = (U^k)^{-1} \cdot \vec{I}^k \quad (4)$$

This results in K intermediate images for each material m . These images are fused to yield the final material images:

$$\vec{J} = \sum_{k=1}^K w_k \cdot \vec{J}^k = \sum_{k=1}^K w_k \cdot (U^k)^{-1} \cdot \vec{I}^k \quad (5)$$

The weights w_k are constant and required to fulfill the boundary condition $\sum_k w_k = 1$ in order to preserve the Hounsfield scale. The values of the w_k are determined by parameter optimization that minimizes the sum of noise variances in the final material images J_m (measured in a representative phantom, e.g. a water phantom with 20 cm diameter).

Multi-energy performance of a research prototype CT scanner with small-pixel counting detector

S. Kappler^{a*}, A. Henning^a, B. Krauss^a, F. Schoeck^a,
K. Stierstorfer^a, T. Weidinger^a, and T. Flohr^a

^aSiemens Healthcare, Siemensstr. 1, 91301 Forchheim, Germany.

$M = 3$ material images calculated from $B = 4$ thresholds

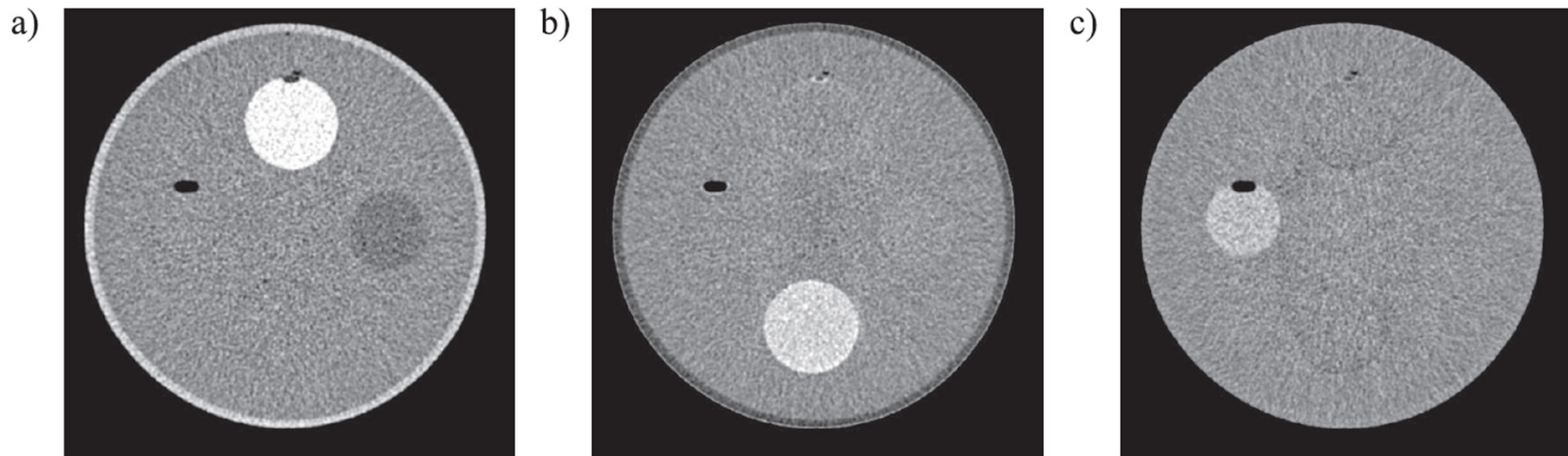


Figure 3. Material decomposed images for calcium (a), iodine (b), and gadolinium (c) created from counting CT data at 140 kVp/100 mA with counter thresholds at 20/35/50/65 keV. The images are displayed in a CT-value window of $C = 0$ and $W = 1200$ HU.

Comparison to Initial Method

- Comparable to the initial method but more expensive since a lot of material images for the different threshold combinations have to be reconstructed and subsequently weighted to get the optimal result.
- The initial method directly finds the optimal weighting coefficients and reconstructs the optimal material image.
- The results of this method should be the same as for the initial method method if the weighting coefficients are chosen optimally, taking the covariance into account.
- Both methods can apply patient specific weighting, although Kappler *et al.* use a water phantom to determine the weighting coefficients.
- Kappler *et al.* work with threshold images, the initial method works with bin images, the results should be the same if the covariance is correctly taken into account.

CT calibration and dose minimization in image-based material decomposition with energy-selective detectors

Sebastian Faby^a, Stefan Kuchenbecker^{a,d}, David Simons^b, Heinz-Peter Schlemmer^b,
Michael Lell^c, and Marc Kachelrieß^{a,d}

^aDivision of Medical Physics in Radiology, German Cancer Research Center (DKFZ),
Im Neuenheimer Feld 280, 69120 Heidelberg, Germany;

^bDivision of Radiology, German Cancer Research Center (DKFZ), Im Neuenheimer Feld 280,
69120 Heidelberg, Germany;

^cDepartment of Radiology, University of Erlangen-Nürnberg, Maximiliansplatz 1,
91054 Erlangen, Germany;

^dInstitute of Medical Physics, University of Erlangen-Nürnberg, Henkestraße 91,
91052 Erlangen, Germany

ABSTRACT

Possible advantages of energy-selective photon counting detectors compared to dual energy CT shall be evaluated in the case of a typical dual energy application: Image-based material decomposition into an iodine and a water material image. Apart from a possibly smaller spectral overlap between the low and the high energy information, a photon counting detector will probably offer more than the two necessary energy bins. In this case additional degrees of freedom are gained that allow minimizing the noise in the material images. We propose an image-based

This is the initial method.

Iterative image-domain decomposition for dual-energy CT

Tianye Niu, Xue Dong, Michael Petrongolo, and Lei Zhu^{a)}

Nuclear and Radiological Engineering and Medical Physics Programs, The George W. Woodruff School of Mechanical Engineering, Georgia Institute of Technology, Atlanta, Georgia 30332

$$\begin{pmatrix} \mu_H \\ \mu_L \end{pmatrix} = \begin{pmatrix} \mu_{1H} & \mu_{2H} \\ \mu_{1L} & \mu_{2L} \end{pmatrix} \begin{pmatrix} x_1 \\ x_2 \end{pmatrix}, \quad (1)$$

where the subscript H (L) indicates the high (low) energy spectrum, and the subscripts 1 and 2 represent the two material bases. In Eq. (1), μ_{ij} is the linear attenuation coefficient of

$$V = \text{diag}(\text{var}(\vec{n}_{H1}), \dots, \text{var}(\vec{n}_{HN}), \text{var}(\vec{n}_{L1}), \dots, \text{var}(\vec{n}_{LN})). \quad (11)$$

In Eq. (11), \vec{n}_{Hk} and \vec{n}_{Lk} are the statistical noise of pixel k in the high-energy and low-energy CT images, respectively. In the derivation of Eq. (10), we assume that the noise is independent on the CT images from two separate scans. Inserting Eq. (10) into Eq. (9), we simplify the framework of iterative decomposition as

$$\min_{\vec{x}} F(\vec{x}) = (A\vec{x} - \vec{\mu})^T V^{-1} (A\vec{x} - \vec{\mu}) + \lambda \cdot R(\vec{x}). \quad (12)$$

boundary sharpness. In this work, we choose the quadratic smoothness penalty function that penalizes the square sum of the differences between one pixel and its nearest horizontal and vertical neighbors.²¹ The penalty function is defined as

$$R(\vec{x}) = \frac{1}{2} \sum_i \sum_{k \in N_i} e_{ik} (x(i) - x(k))^2, \quad (13)$$

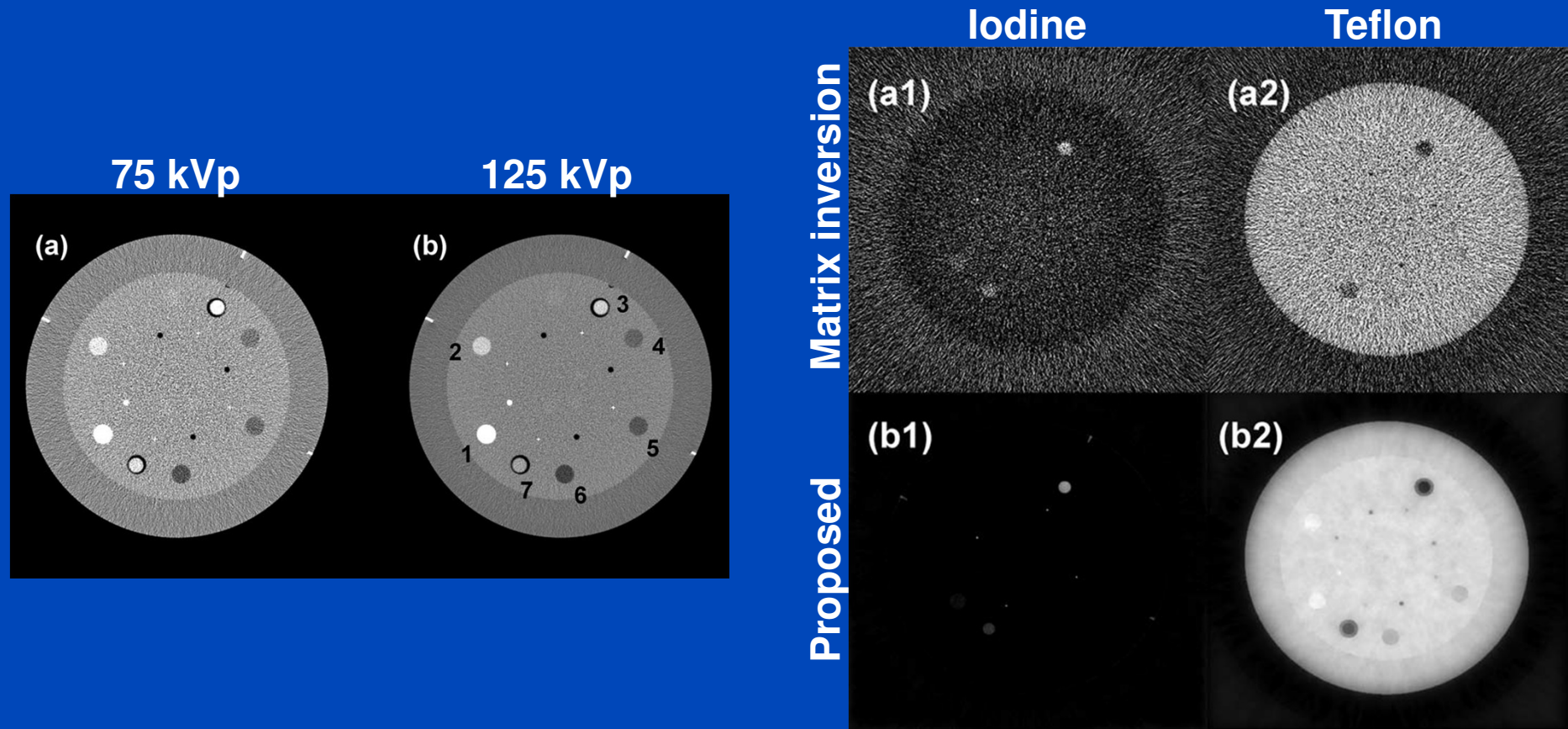
where N_i is the set of the four neighbors of the i th pixel in the image. e_{ik} is the edge-detection weight, which is a small value if either i or k is the index of an edge pixel in the image and one otherwise.²¹ In this work, we set the weight to be 0.1 in

Iterative image-domain decomposition for dual-energy CT

Tianye Niu, Xue Dong, Michael Petrongolo, and Lei Zhu^{a)}

Nuclear and Radiological Engineering and Medical Physics Programs, The George W. Woodruff School of Mechanical Engineering, Georgia Institute of Technology, Atlanta, Georgia 30332

Dual energy results, $B = 2$ and $M = 2$



Comparison to Initial Method

- Iterative material decomposition with a decomposition matrix approach plus edge-preserving regularization on the material images
- Independent treatment of the two material images
- $B = M$, i.e. no considerations regarding more bins than materials
- Only for DECT

Spectral diffusion: an algorithm for robust material decomposition of spectral CT data

Darin P Clark and Cristian T Badea

Center for *In Vivo* Microscopy, Box 3302, Duke University Medical Center, Durham, NC 27710, USA

Post-reconstruction material decomposition solves the following least-squares optimization problem:

$$C = \arg \min_C \frac{1}{2} \| C - DX \|_2^2. \quad (1)$$

Given the input spectral CT data, X , the objective is to find the material decomposition, C . In the case where the number of CT data sets matches the number of materials, D and D^T perform material decomposition (spectral data, X , to material maps, C ; equation (2)) and synthesis (material maps to spectral data; equation (3)) using a sensitivity matrix, B :

$$DX = B^{-1}X = \begin{bmatrix} b_{I,E1} & b_{Au,E1} & b_{Gd,E1} \\ b_{I,E2} & b_{Au,E2} & b_{Gd,E2} \\ b_{I,E3} & b_{Au,E3} & b_{Gd,E3} \end{bmatrix}^{-1} \begin{bmatrix} X_{E1} \\ X_{E2} \\ X_{E3} \end{bmatrix} = C \quad (2)$$

$$D^T C = BC = \begin{bmatrix} b_{I,E1} & b_{Au,E1} & b_{Gd,E1} \\ b_{I,E2} & b_{Au,E2} & b_{Gd,E2} \\ b_{I,E3} & b_{Au,E3} & b_{Gd,E3} \end{bmatrix} \begin{bmatrix} C_I \\ C_{Au} \\ C_{Gd} \end{bmatrix} = X = D^T DX \quad (3)$$

The objective of spectral diffusion is summarized by the following optimization problem:

$$X = \arg \min_X \frac{1}{2} \| X - Y \|_2^2 + \mu_1 \Gamma(X) + \mu_2 \Gamma(DX). \quad (18)$$

Given the input data, Y , the objective is to find a denoised version of the data, X , which best minimizes the cost specified by $\Gamma(\cdot)$ for both the data and the material decomposition of the data, DX , while maintaining data fidelity. The relative contribution of each term is controlled by the regularization parameters μ_1 and μ_2 . A popular choice for Γ when working with

(BTV, (Farsiu *et al* 2004)). As the name suggests, BTV is related to the previously discussed bilateral filtration (BF) weights in the following way:

$$R(x, y) = \exp\left(-\frac{(f(x, y) - \langle K(y), f(x, y) \rangle)^2}{2m^2\sigma^2}\right) = \exp\left(-\frac{(W(y)X(x, y) - \langle W(y)X(x, y) \rangle)^2}{2m^2\sigma^2}\right) \quad (20)$$

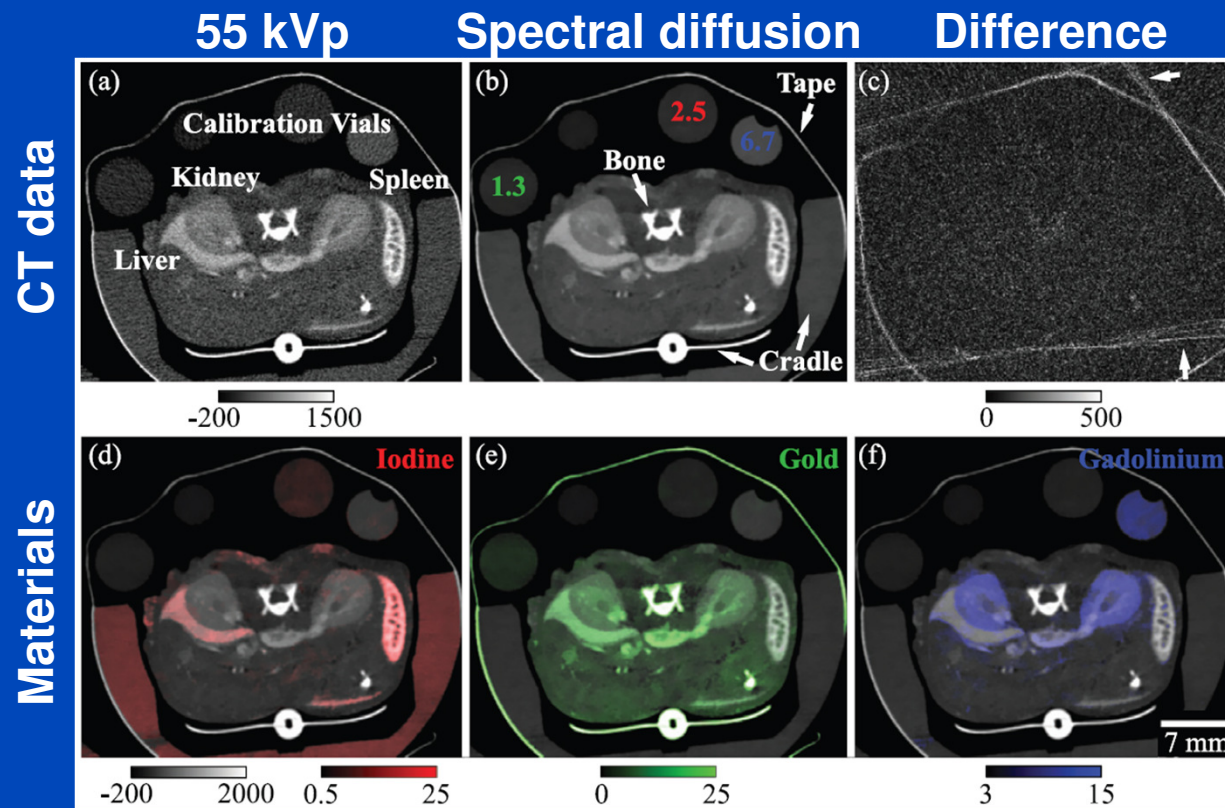
$$\Gamma_{\text{BTV}}(X) = \left\| \frac{\sum_{y=1}^I D(y) R(x, y) |W(y)X(x, y)|}{\sum_{y=1}^I D(y) R(x, y)} \right\| \quad (21)$$

Spectral diffusion: an algorithm for robust material decomposition of spectral CT data

Darin P Clark and Cristian T Badea

Center for *In Vivo* Microscopy, Box 3302, Duke University Medical Center, Durham, NC 27710, USA

Results for $B = 3$ (40 kVp, 55 kVp, 140 kVp) and $M = 3$



Comparison to Initial Method

- Iterative material decomposition with edge-preserving regularization on both the energy-resolved input images and the material images
- Yields denoised material images AND denoised energy-resolved CT images
- Joint treatment of the energy-resolved input images
- No considerations regarding more bins than materials

Image-based Material Decomposition with a General Volume Constraint for Photon-Counting CT

Zhoubo Li^a, Shuai Leng^b, Lifeng Yu^b, Zhicong Yu^b, Cynthia H. McCollough^{*a,b}

^aDepartment of Biomedical Engineering and Physiology, Mayo Clinic College of Medicine, Rochester, MN 55905; ^bDepartment of Radiology, Mayo Clinic, Rochester, MN 55905

ii. Conversion between CT number and linear attenuation coefficient: The proposed method directly works on CT number, assuming the relationship between CT number and line attenuation coefficient is

$$CT = \frac{\mu - \mu_w}{\mu_w} \times 1000. \quad (2)$$

Combining Eqs. (1) and (2), one can derive the system equation for multi-energy CT measurement:

$$CT(E) = CT(E)_1 \frac{\hat{\rho}_1}{\rho_1} + CT(E)_2 \frac{\hat{\rho}_2}{\rho_2} + \dots + CT(E)_N \frac{\hat{\rho}_N}{\rho_N} + 1000(\delta - 1) \quad (3)$$

and a general condition on volume constraint in the mixture:

$$\delta = \frac{\hat{\rho}_1}{\rho_1} + \frac{\hat{\rho}_2}{\rho_2} + \dots + \frac{\hat{\rho}_N}{\rho_N} = \frac{V_1}{\hat{V}} + \frac{V_2}{\hat{V}} + \dots + \frac{V_N}{\hat{V}}, \quad (4)$$

where $\hat{\rho}_i$ (\hat{V}) is the concentration (Volume) of basis material i in the mixture and ρ_i (V_i) is its concentration (Volume) in its pure form. $CT(E)_i$ represents the CT number of basis material i in its pure form at energy E . Here δ is a variable which depends on the composition of basis materials. It can be smaller or bigger than 1. When it is equal to 1, the proposed method is identical to methods with volume conservation. An example where $\delta > 1$ is a mixture of iron chloride (FeCl_3) and water, which will have a decreased volume relative to the sum of the individual component volumes. Examples where $\delta < 1$ include some biopolymer-water solution, which can have a total volume that is greater than the sum of the individual component volumes.

One can further rearrange (3) and (4) into a matrix form

$$\begin{bmatrix} CT(E_1) \\ \vdots \\ CT(E_M) \\ 1000 \end{bmatrix} = \begin{bmatrix} CT(E_1)_1/\rho_1 & \dots & CT(E_1)_N/\rho_N & 1000 \\ \vdots & \vdots & \vdots & \vdots \\ CT(E_M)_1/\rho_1 & \dots & CT(E_M)_N/\rho_N & 1000 \\ 1000/\rho_1 & \dots & 1000/\rho_N & -1000 \end{bmatrix} \begin{bmatrix} \hat{\rho}_1 \\ \vdots \\ \hat{\rho}_N \\ \delta - 1 \end{bmatrix}. \quad (5)$$

The proposed method determines basis material concentration by solving the following inversion equation:

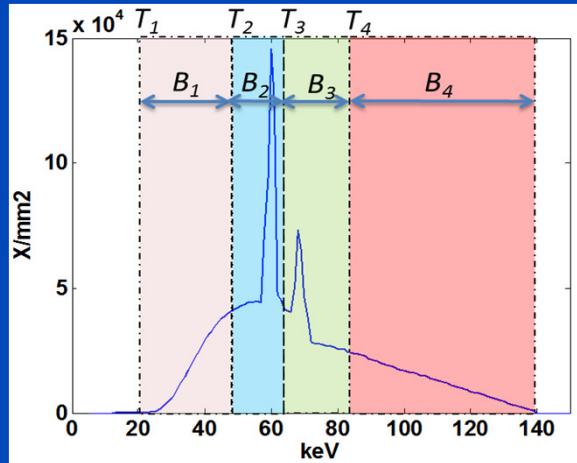
$$[\hat{\rho}] = [M]^{-1}[CT], \quad (6)$$

where $\hat{\rho}$ is the unknown basis material and mixture densities, M is a material matrix associated with the attenuation properties of the basis materials, and $[CT]$ is the matrix of multi-energy CT measurement in Hounsfield unit.

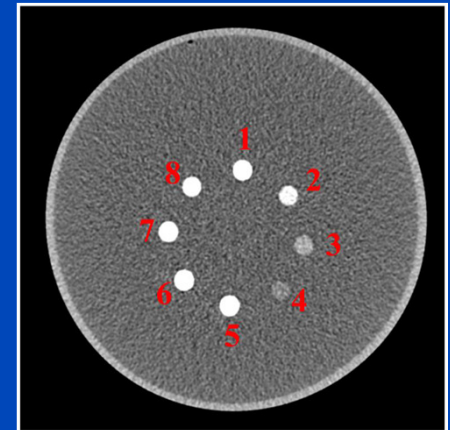
Image-based Material Decomposition with a General Volume Constraint for Photon-Counting CT

Zhoubo Li^a, Shuai Leng^b, Lifeng Yu^b, Zhicong Yu^b, Cynthia H. McCollough^{*a,b}

^a Department of Biomedical Engineering and Physiology, Mayo Clinic College of Medicine, Rochester, MN 55905; ^b Department of Radiology, Mayo Clinic, Rochester, MN 55905



Results for $B = 4$ and $M = 3$

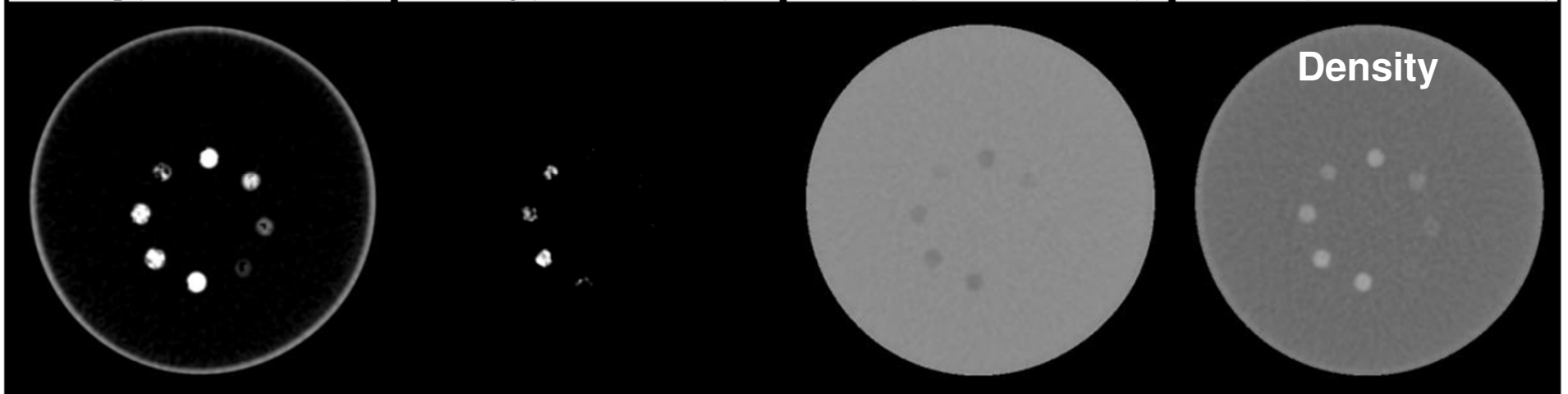


CaCl₂ (W/L = 200/120)

FeCl₃ (W/L = 140/80)

Water (W/L = 1200/950)

Mixture (W/L = 1100/1100)



Comparison to Initial Method

- **Material decomposition with an additional volume constraint to allow the separation of more than two materials without pronounced K-edge**
- **Constrained least-squares fitting based on prior information to reduce noise in the material images and to make use of the energy bin redundancy (unfortunately no details in the paper regarding this step)**
- **No statistical considerations regarding more bins than materials**

Methods Overview

Authors	Method	Post Processing	B > M	Comments
Schlomka ¹ 2008	Maximum Likelihood	No	Yes	rawdata-based (i.e. non-linear)
Schmidt 2009	Error propagation	No	-	CNR optimization
Maaß et al. ^{2,3} 2011	Bin combinations + Error propagation	No	Yes	rawdata-based (i.e. non-linear)
Alvarez ⁴ 2011	ML-based LUT	No	Yes	rawdata-based (i.e. non-linear)
Kappler et al. 2013	Bin combinations + Error propagation	No	Yes	
Faby et al. 2014	SVD + Error propagation	No	Yes	Initial method (of this presentation)
Niu et al. 2014	Denoising	Yes	No	B=M=2, DECT only
Clark and Badea 2014	Spectral diffusion	Yes	No	
Li et al. 2015	Rank M+1 solution only, no null space	No	Yes	volume constraint (i.e. M+1 materials)

¹ Schlomka et al. "Experimental feasibility of multi-energy photon-counting K-edge imaging in pre-clinical computed tomography", PMB 2008. ^{2,3} Maaß, Sawall, Kachelrieß. "Empirical multi-energy calibration (EMEC) for material-selective CT" and "Dose minimization for material-selective CT with energy-selective detectors". IEEE MIC Record, 2011. ⁴ Alvarez. "Estimator for photon counting energy selective x-ray imaging with multibin pulse height analysis" MedPhys 2011.

Thank You!



The 4th International Conference on Image Formation in X-Ray Computed Tomography

July 18 – July 22, 2016, Bamberg, Germany
www.ct-meeting.org



Conference Chair

Marc Kachelrieß, German Cancer Research Center (DKFZ), Heidelberg, Germany

This presentation will soon be available at www.dkfz.de/ct.
Parts of the reconstruction software were provided by RayConStruct[®] GmbH,
Nürnberg, Germany.